International Journal of Nanomedicine

Dovepress
open access to scientific and medical research

Open Access Full Text Article

ORIGINAL RESEARCH

Sn doping induced enhancement in the activity of ZnO nanostructures against antibiotic resistant *S. aureus* bacteria

This article was published in the following Dove Press journal:
International Journal of Nanomedicine
27 September 2013
Number of times this article has been viewed

Tariq Jan[1]
Javed Iqbal[1]
Muhammad Ismail[2]
M Zakaullah[3]
Sajjad Haider Naqvi[4]
Noor Badshah[5]

[1]Laboratory of Nanoscience and Technology, Department of Physics, International Islamic University, Islamabad, Pakistan; [2]Institute of Biomedical and Genetic Engineering, Islamabad, Pakistan; [3]Department of Physics, Quaid-i-Azam University, Islamabad, Pakistan; [4]Department of Biochemistry, University of Karachi, Karachi, Pakistan; [5]Department of Basic Science, University of Engineering and Technology, Peshawar, Pakistan

Abstract: Highly ionic metal oxide nanostructures are attractive, not only for their physiochemical properties but also for antibacterial activity. Zinc oxide (ZnO) nanostructures are known to have inhibitory activity against many pathogens but very little is known about doping effects on it. The antibacterial activity of undoped ZnO and tin (Sn) doped ZnO nanostructures synthesized by a simple, versatile, and wet chemical technique have been investigated against *Escherichia coli*, methicillin-resistant *Staphylococcus aureus*, and *Pseudomonas aeruginosa* bacterial strains. It has been interestingly observed that Sn doping enhanced the inhibitory activity of ZnO against *S. aureus* more efficiently than the other two bacterial strains. From cytotoxicity and reactive oxygen species (ROS) production studies it is found that Sn doping concentration in ZnO does not alter the cytotoxicity and ROS production very much. It has also been observed that undoped and Sn doped ZnO nanostructures are biosafe and biocompatible materials towards *SH-SY5Y* Cells. The observed behavior of ZnO nanostructures with Sn doping is a new way to prevent bacterial infections of *S. aureus*, especially on skin, when using these nanostructures in creams or lotions in addition to their sunscreen property as an ultraviolet filter. Structural investigations have confirmed the formation of a single phase wurtzite structure of ZnO. The morphology of ZnO nanostructures is found to vary from spherical to rod shaped as a function of Sn doping. The excitation absorption peak of ZnO is observed to have a blue shift, with Sn doping leading toward a significant tuning in band gap.

Keywords: nanostructures, Sn doped ZnO, *S. aureus*, antibacterial activity

Introduction

Zinc oxide (ZnO) is a semiconductor with large excitation binding energy (60 meV), direct wide energy band gap (3.37 eV), good chemical and thermal stability, p-type electrical conductivity, and is abundant in nature, nontoxic, and environmentally friendly.[1,2] These tremendous properties make this material attractive for many applications such as electronic and optoelectronic devices, electrochemical devices, solar cells, and photo catalysis.[3] At nanoscale, ZnO demonstrates unique physical and chemical properties because of its high aspect ratio of atoms (ie, surface to volume ratio). ZnO nanostructures have vast applications such as dye sensitized solar cells, field effect transistors, targeted drug delivery, anticancer agents, and antibacterial activity.[4–8] Recently, it has been reported that the doping of ZnO nanostructures with other elements can enhance its various properties.[9] Commonly, different elements as a dopant in ZnO can be categorized into two groups: one group can substitute for zinc (Zn) and the second group for oxygen (O). These different dopants can tune various properties of ZnO nanostructures. Tin (Sn) as a cation dopant can substitute for Zn and tailor various properties of ZnO.[10]

Correspondence: Javed Iqbal
Laboratory of Nanoscience and Technology, Department of Physics, International Islamic University, Islamabad, 44000 Pakistan
Tel +92 51 901 9713
Fax +92 51 925 7954
Email javed.saggu@iiu.edu.pk

The recurrence of infectious diseases and continuous development of resistance among the diversity of disease causing bacteria poses a stern threat to public health worldwide.[11,12] Among these, *Escherichia coli*, *Staphylococcus aureus*, and *Pseudomonas aeruginosa* are the common species that can cause a wide variety of infections and diseases.[13,14] Mortality and morbidity linked with these bacteria remain high regardless of antimicrobial therapy, partially because these species develop resistance capability to antibiotics. Therefore, new strategies are highly desired to identify and to develop a new generation of agents against these species. ZnO nanostructures are of particular interest due to their low cost, nontoxic nature, their abundance in nature, and established use in health care products.[15,16] Recently, it is reported that Sn doping has significantly enhanced the antibacterial activity of titanium dioxide (TiO_2) nanoparticles.[17] But the use of TiO_2 is limited due to its allergic reactions to sensitive skin.[17] However, ZnO is known to have significant activity against various microorganisms and does not cause any allergic reactions on the skin by dispersing the light falling on it.[18] In this study, undoped and Sn doped ZnO nanostructures have been fabricated by a simple coprecipitation technique and the influence of Sn doping on the antibacterial activity and physiochemical properties of ZnO nanostructures is studied in detail.

Materials and methods

Synthesis of Sn doped ZnO nanostructures

For synthesis of undoped ZnO and Sn doped ZnO nanostructures, zinc chloride ($ZnCl_2$), $SnCl_4$-$5H_2O$, and sodium hydroxide (NaOH) (Sigma-Aldrich, St Louis, MO, USA) were used. All chemicals were of analytical grade and used without further purification. The synthesis was performed by a simple coprecipitation technique using distilled water as a solvent. For synthesis of undoped ZnO nanostructures, a 0.1 M solution of $ZnCl_2$ in distilled water was stirred up to 20 minutes for complete dissolution. Then, a 1 M NaOH solution in distilled water was added to the above solution drop by drop and the pH value was adjusted to approximately 8. After adjusting the pH value, the solution was stirred for 1 hour. Precipitates were collected from the solution by centrifugation. For Sn doping, the same procedure was adopted except for the addition of $SnCl_4$-$5H_2O$ at various molar ratios to $ZnCl_2$ for 2%, 4%, and 6% Sn doping. All samples were dried in an oven for 5 hours at 80°C and then ground to a powder. The samples were annealed in a chamber furnace for 2 hours at 600°C. The synthesized samples crystallinity, morphology, optical bandgap, and absorption of light were examined using X-ray diffraction (XRD), scanning electron microscopy (SEM), transmission electron microscopy (TEM), UV-visible spectroscopy and Fourier transform infrared spectroscopy (FTIR) respectively.

Preparation of master solution

A preset amount of undoped and Sn doped ZnO nanostructures were mixed with sterilized water separately with the help of a magnetic stirrer. After complete dissolution of nanostructures, the solutions were placed in an ultrasonicator to deagglomerate the nanostructures. After 30 minutes of sonication, the so- called dispersed undoped and Sn doped ZnO nanostructures were prepared and had a concentration of 2 mg/mL.

Determination of antibacterial activity of nanostructures

Activity of synthesized nanostructures were examined against; *E. coli, Pseudomonas aeruginosa* and *S. aureus*. All strains were grown aerobically at 37°C under normal laboratory light conditions.

For the antibacterial assay, the above mentioned microorganisms were grown in a liquid media (nutrient broth media) in the presence of a colloidal suspension of undoped and Sn doped ZnO nanostructures. The cultures without nanostructures colloidal suspension grown under the same conditions were considered as the control. The growth of these microbial colonies was monitored by measuring optical density at 2 hour intervals under a UV-visible spectrophotometer at a wavelength of 600 nm.

The in vitro antibacterial activity of the synthesized undoped and Sn doped ZnO nanostructures were investigated by the disc method. Single colonies of *E. coli*, *S. aureus,* and *P. aeruginosa* were cultured in agar medium by lawn formation. The colloidal suspension of nanostructures was applied to agar petri plates by the disc method. These agar plates were incubated at 37°C for 24 hours and the zone of inhibition was measured in millimeters.

Cell culture and treatment with ZnO nanostructures

The SH-SY5Y human cell line was purchased from American Type Culture Collection (Manassas, VA, USA). Cells were maintained in Dulbecco's Modified Eagle's Medium (DMEM) (Sigma-Aldrich) supplemented with 10% fetal bovine serum (FBS) and grown at 37°C in a humidified environment with 5% CO_2 plus 95% air. Cells were seeded in 96 well plates and allowed to attach for 48 hours. The suspensions of ZnO

nanostructures doped with different Sn concentrations were applied to the cells. Cells without Sn doped ZnO nanostructures were used as the control in these experiments. A fluorescence microscope (Hitachi, Tokyo, Japan) was used for the cell viability assay and flow cytometry was used for reactive oxygen species (ROS) detection.

Results and discussion

To study the influence of Sn doping on the structural properties of ZnO nanostructures, XRD analysis of undoped and Sn doped ZnO nanostructures has been carried out with step size of 0.2° (2 θ) and 2θ range of 20°–70° with CuK_{α} radiation having wavelength 1.54Å. Figure 1 shows the XRD patterns for undoped and Sn doped ZnO nanostructures. The broadness of the peaks in XRD patterns shows the nanocrystalline nature of all prepared samples. All peaks are indexed to (100), (002), (101), (102), (110), (103), (200), (112), and (201) planes which corresponds to the typical hexagonal wurtzite structure of ZnO. This is in agreement with reported literature and the standard pattern of ZnO.[19] The absence of extra peaks related to Sn or other impurities in the XRD patterns with Sn doping confirms the phase purity of all synthesized samples. There is a shift toward higher angle and a decrease in the full width half maximum value with Sn doping, as shown in Figure 2, which confirms the successful incorporation of Sn into the ZnO lattice and the reduction of strain.[20] The particle sizes have been calculated from the broadening of the main peak (101) using Scherrer's formula for undoped and Sn doped ZnO samples. The average sizes of particles are 17 nm, 24 nm, 32 nm, and 36 nm for undoped, 2%, 4%, and 6% Sn doped ZnO, respectively. The increase

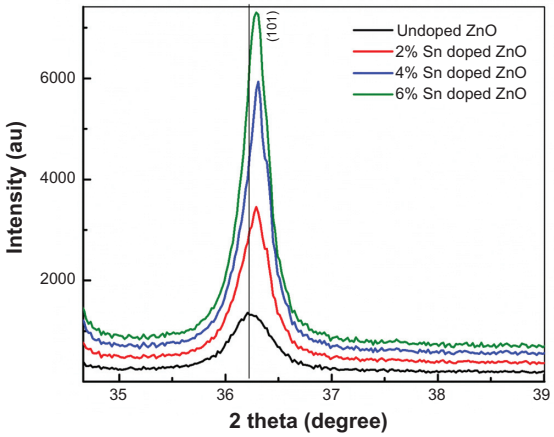

Figure 2 Extended X-ray diffraction patterns of undoped and tin doped zinc oxide nanostructures.
Abbreviations: Sn, tin; ZnO, zinc oxide.

in particle size as a function of Sn doping may be attributed to the fact that ionic radii of Sn^{4+} may be larger than Zn^{2+} (0.74Å), which means that the coordination number of Sn^{4+} in the crystal would be greater than 4 (0.69Å for 4-coordinate, 0.83Å for 6-coordinate, and 0.95 for 8-coordinate).[21] The increase in particle size with Sn doping in the ZnO lattice clearly demonstrates improvement in the crystallinity of the synthesized samples.

The morphological examination of undoped ZnO and Sn doped ZnO samples was done by SEM. Figure 3 shows SEM micrographs of undoped ZnO and Sn doped ZnO samples. It can be observed from the figure that the morphology of ZnO samples is spherical and changes from spherical to rods with Sn doping. The morphological variation may be due to the huge influence of Sn ion doping on ZnO nanostructures and

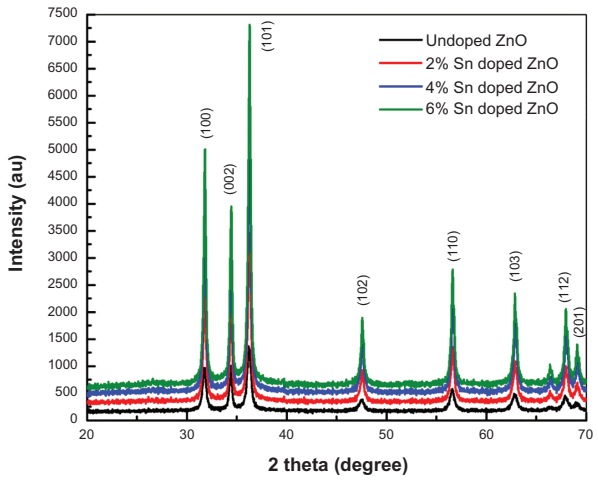

Figure 1 X-ray diffraction patterns of undoped and tin doped zinc oxide nanostructures.
Abbreviations: Sn, tin; ZnO, zinc oxide.

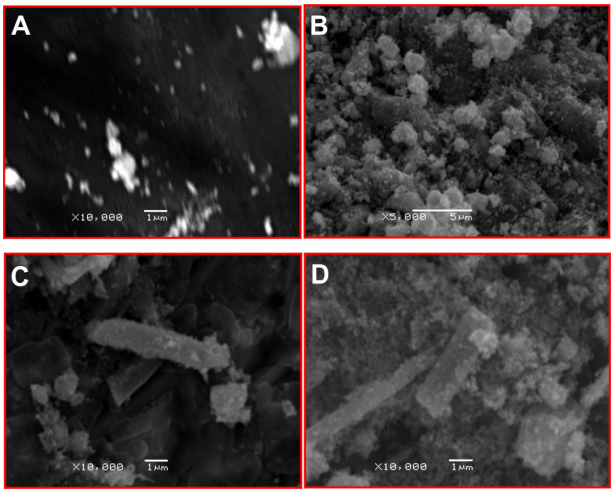

Figure 3 Scanning electron micrographs of undoped and tin doped zinc oxide.
Notes: (**A**) undoped, (**B**) 2% tin (Sn), (**C**) 4% Sn, and (**D**) 6% Sn doped zinc oxide.

dipolar interaction along the c-axis with the Sn^{4+} substitution to Zn^{2+}. Moreover, there is an increase in grain size as a function of increase in Sn dopant concentration. This variation in grain size may be due to the aggregation of small particles into large grains during annealing of samples at 600°C.

The morphologies of undoped and Sn doped ZnO nanostructures were further investigated by transmission electron microscope (TEM). TEM micrographs of undoped ZnO nanoparticles show nearly spherical particles with an average size of 47 nm as shown in Figure 4A. Figure 4B represents a TEM micrograph of 4% Sn doped ZnO nanostructures with particle and rod mixed morphologies. It is demonstrated by the TEM results that both particle size and morphology are greatly influenced by Sn doping into ZnO matrix. The particle size distribution is shown in Figure 4C.

UV-visible absorption spectroscopy is an important technique to investigate the optical properties of nanoparticles. To examine the influence of Sn doping on the optical properties of ZnO nanostructures, UV-visible absorption spectroscopy of undoped ZnO and Sn doped ZnO nanostructures was performed and the results are shown in Figure 5. A typical excitation absorption band at 378 nm is observed for undoped ZnO nanostructure which has a blue shift when compared to that of bulk ZnO.[22] It can be observed from Figure 5 that the excitation absorption band has a further blue shift with increases in Sn concentration as a dopant into ZnO. As can be depicted from the XRD and SEM results that particle size increases with the increase in Sn concentration, this blue shift may be attributed to quantum size effects.

Nanostructures have a very high aspect ratio (ie, surface to volume ratio) when compared to their bulk counterpart. This property makes nanostructures more chemically reactive, because more atoms are accommodated on the surface. Therefore, knowing the surface chemistry of samples that have been synthesized is of immense interest. To study the presence or absence of various vibration modes and to investigate the influence of Sn doping on ZnO nanostructures, FTIR spectroscopy of undoped ZnO and Sn doped ZnO nanostructures was performed. Figure 6 shows the FTIR transmission mode spectra of undoped ZnO and Sn doped

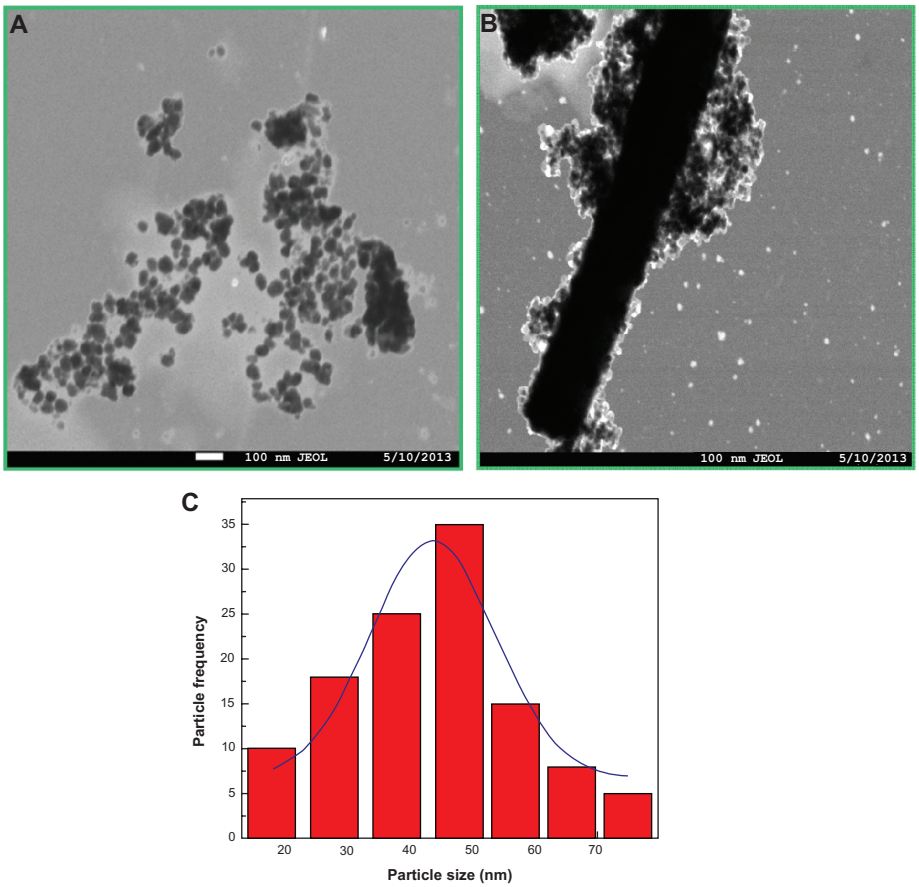

Figure 4 TEM micrographs of tin doped zinc oxide nanostructures.
Notes: (**A**) 0%, (**B**) 4%, and (**C**) particle size distribution histogram with Gaussian fit of undoped zinc oxide.
Abbreviation: TEM, transmission electron microscope.

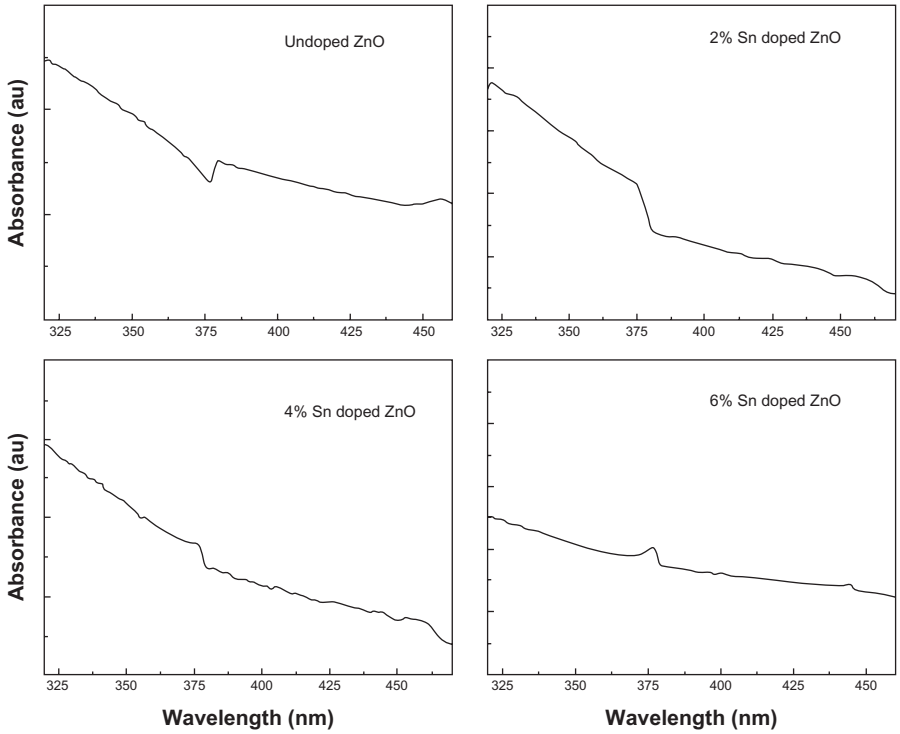

Figure 5 Ultraviolet-visible absorption spectra of undoped zinc oxide and tin doped zinc oxide nanostructures.
Abbreviations: Sn, tin; ZnO, zinc oxide.

ZnO nanostructures. The spectrum of each sample shows a series of absorption peaks from 400 to 4000 cm^{-1}. The broad peak at approximately 3360 cm^{-1} in all samples can be assigned to the presence of hydroxyl groups on the surface of samples. The peaks around 1500–1600 cm^{-1} are due to the presence of C=O stretching mode on the surfaces of the samples. In Figure 6, the characteristic peak of ZnO occurs at approximately 412 cm^{-1}, which confirms the formation of ZnO. In infrared region, when morphology of particles changes from spherical particles to needle like structures, spectra often show two absorption maxima.[23] In our case, when the particle morphology changes from spherical to rods, two absorption peaks are observed at approximately 412 cm^{-1} and 695 cm^{-1} for ZnO.

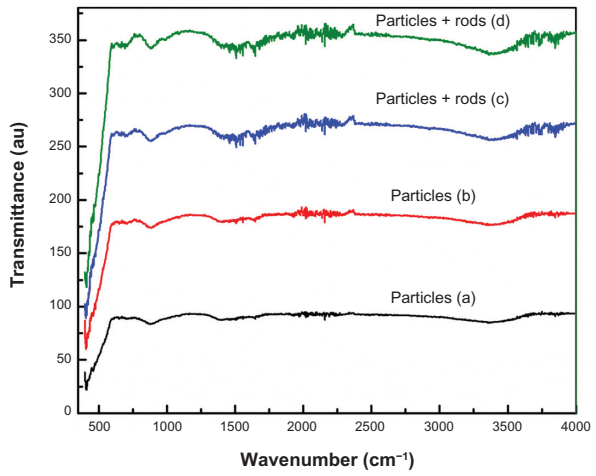

Figure 6 Fourier transform infrared spectroscopy spectra of zinc oxide nanostructures.
Notes: (**a**) undoped zinc oxide (ZnO), (**b**) 2% tin (Sn) doped ZnO, (**c**) 4% Sn doped ZnO, and (**d**) 6% Sn doped ZnO nanostructures.

The influence of Sn doping on the activity of ZnO nanostructures against *E. coli*, *S. aureus*, and *P. aeruginosa* microbial colony growth was investigated. Figure 7 (A-C) shows the effect of undoped and Sn doped ZnO nanostructures on the growth rate of *E. coli*, *S. aureus*, and *P. aeruginosa*, respectively. It was observed that all the synthesized samples effectively inhibited the growth rate of *S. aureus* but are less effective against the other two bacterial strains tested. The antibacterial activity is probably derived from the interaction of negatively charged cell membranes and positively charged nanostructures, interaction of metal ions with bacteria, and the orientation of nanostructures.[24] Sn doping influenced the activity of ZnO nanostructures against all the bacterial strains tested. The efficacy of ZnO nanostructures against growth inhibition of these bacterial strains varies slightly with increases in Sn concentration.

The in vitro activity of undoped and Sn doped ZnO nanostructures toward different bacterial pathogens were investigated by the disc diffusion agar method. All samples

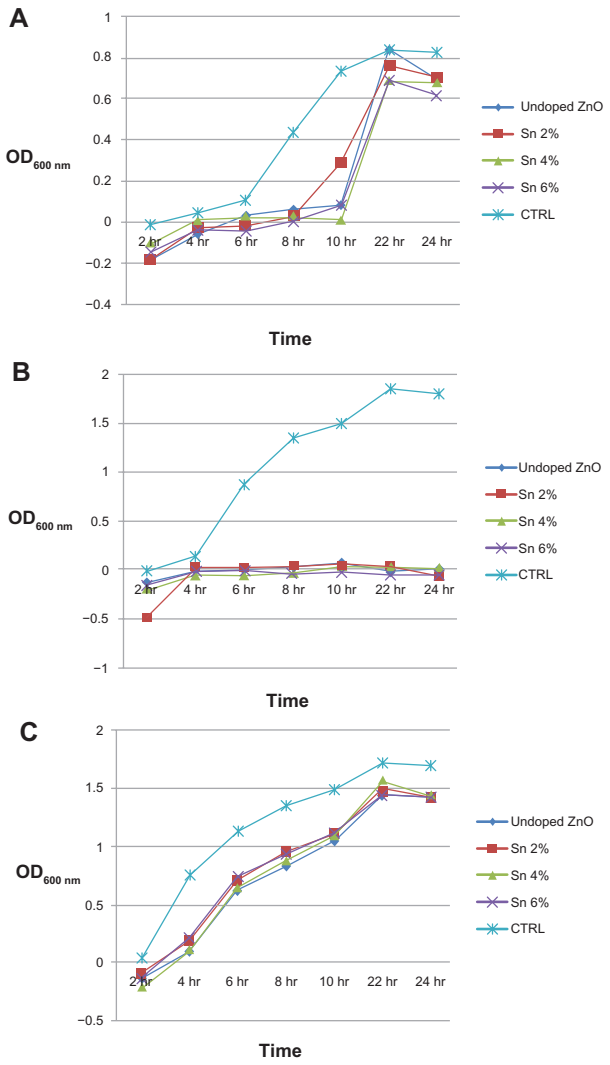

Figure 7 Effect of undoped and tin doped zinc oxide nanostructures on bacteria growth.

Notes: (**A**) Effect of undoped and tin (Sn) doped zinc oxide (ZnO) nanostructures on the growth rate of *Escherichia coli* strain. (**B**) Effect of undoped and Sn doped ZnO nanostructures on the growth rate of *Staphylococcus aureus* strain. (**C**) Effect of undoped and Sn doped ZnO nanostructures on the growth rate of *Pseudomonas aeruginosa* strain.

Abbreviations: Sn, tin; ZnO, zinc oxide; OD, optical density; CTRL, control.

show antibacterial activity toward all three pathogens, as shown in Figure 8. Interestingly, the zone of inhibition produced by undoped ZnO is higher than that of 2% Sn doped ZnO, but less than that of 4% Sn doped ZnO, and the inhibition zone caused by 6% Sn doped ZnO is less than that of 4% Sn doped ZnO against all the three types of pathogens, as shown in Figure 9. It is demonstrated in the reported literature that particle size and morphology greatly influence the activity of ZnO against various microorganisms.[25–27] In this study, both particle size and shape seem to play a vital role in the activity of ZnO against all the three pathogens. The antibacterial activity of ZnO nanostructures may be attributed to several mechanisms such as electrostatic interactions of cell walls and membranes, generation of ROS, and medium.[27] In this study, the antibacterial activity of undoped ZnO is higher when compared to 2% Sn doped ZnO, because particle size is lesser in the first case. But the inhibitory activity of 4% Sn doped ZnO is higher than that of undoped and 2% Sn doped ZnO, though particle size of 4% Sn doped ZnO is larger than the undoped and 2% Sn doped ZnO. From SEM results, it has been observed that the morphology of the 4% Sn doped ZnO was rod shaped, while that of the undoped and the 2% Sn doped ZnO was spherical. The inhibitory activity of 6% Sn doped ZnO is less than that of the 4% Sn doped ZnO. This may be due to the reason that the particle size is greater in case of 6% Sn doped ZnO. It may be concluded that particle size, Sn content, and morphology play vital roles in the activity of undoped and Sn doped ZnO nanostructures against all the pathogens tested.

Sn doping has significantly enhanced the activity of ZnO against *S. aureus* when compared to the other two bacterial strains tested. The zone of inhibition produced by 4% Sn doped ZnO is 22 mm, which is almost 37% more than that produced by undoped ZnO nanostructures (14 mm), as shown in Figure 9. *S. aureus* is a bacterium responsible for various skin diseases which are hard to treat with traditional antibiotics. *S. aureus* can also easily contaminate hospital implants and thereby spread and cause various serious infections.[27,28] ZnO is a well known material due to its established use in creams, lotions, antibacterial coatings, and UV protectors. Therefore, using 4% Sn doped ZnO nanostructures instead of ZnO in UV protectors, creams, and lotions will lead to effective control of bacterial infections in addition to their UV blocking properties.[15,27] Also, spreading of infectious diseases due to bacterial contamination may be controlled by coating hospital implants with Sn doped ZnO nanostructures. Therefore, it is strongly recommended that the use of 4% Sn doped ZnO nanostructures, instead of undoped ZnO, may have more potential applications.

To evaluate the cytotoxicity of Sn doped ZnO nanostructures, SH-SY5Y cells grown in DMEM with 10% FBS were exposed to ZnO nanostructures doped with different Sn concentrations (2%, 4%, and 6%) for 24 hours and its effect on SH-SY5Y cells was tested. To investigate if Sn doped ZnO nanostructures support cell survival, we performed optical microscopy and quantified the total cell number with and without Sn doped ZnO nanostructures. It is shown in Figure 10A that there is no significant effect of undoped ZnO and Sn doped ZnO nanostructures on the SH-SY5Y cells. All synthesized samples may be considered as biosafe because the percentage of damage is very low.

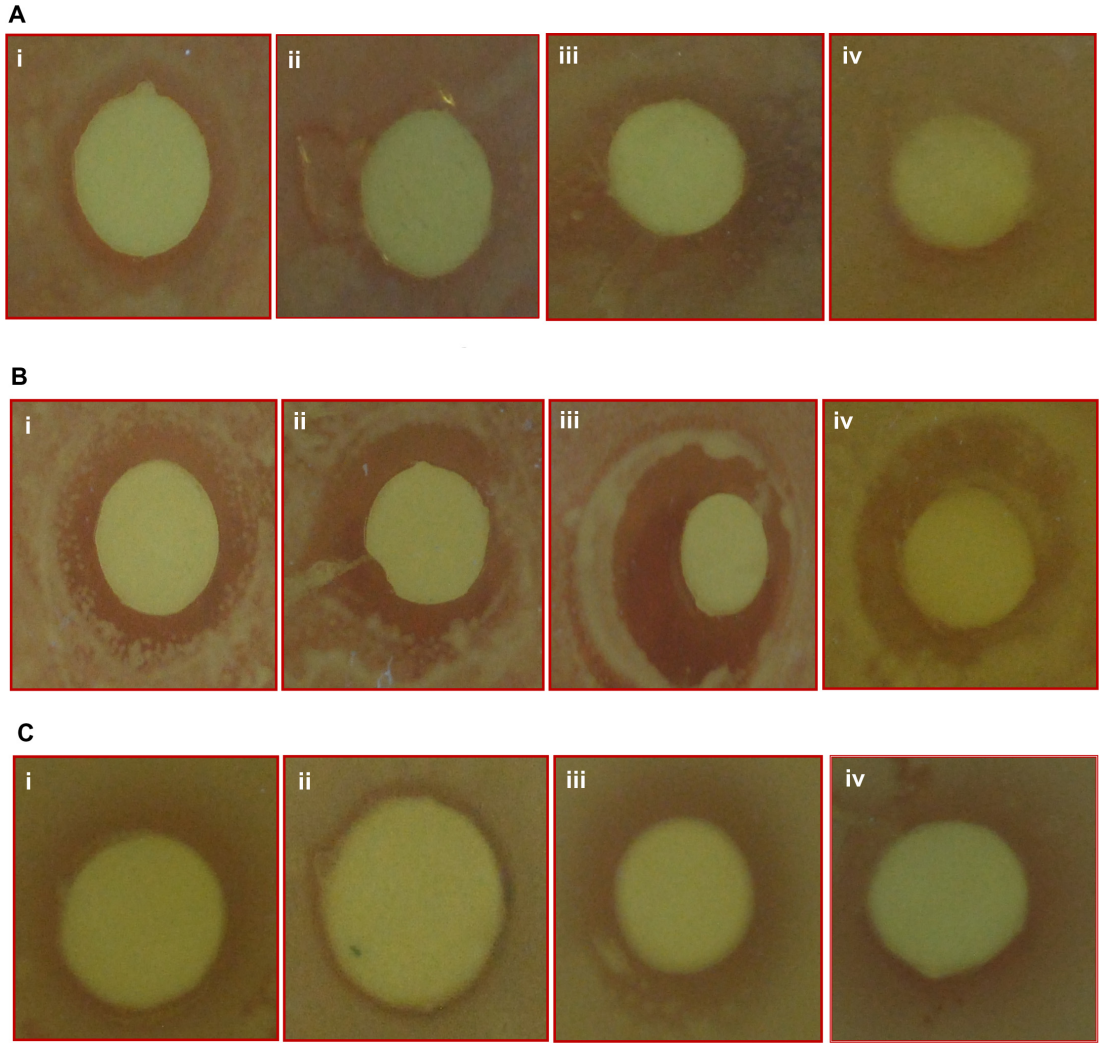

Figure 8 Zone of inhibition produced by undoped and Sn doped ZnO nanostructures.
Notes: (i) 0%, (ii) 2%, (iii) 4%, and (iv) 6% Sn doped ZnO against different bacterial strains ie, (**A**) *Escherichia coli,* (**B**) *Staphylococcus aureus* and (**C**) *Pseudomonas aeruginosa.*
Abbreviations: Sn, tin; ZnO, zinc oxide.

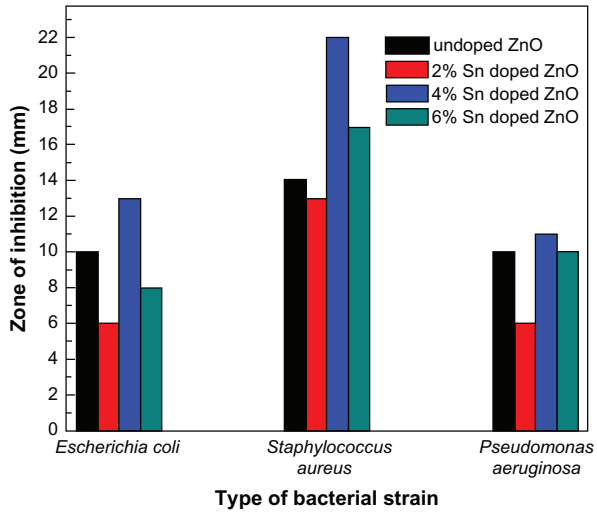

Figure 9 Bar graphs showing zone of inhibitions introduced by undoped and tin doped zinc oxide nanostructures against various bacterial strains.
Abbreviations: Sn, tin; ZnO, zinc oxide.

To further evaluate the biosafety and biocompatibility of Sn doped ZnO nanostructures, its reactive oxygen species (ROS) generation study was conducted. The toxicological effect of reactive oxygen species and the resulting oxidative stress has been extensively studied with reference to engineered nanostructures. The production of ROS could be resulted at particle surface because of the semi-conducting or the electronic properties of the material. It might also be related to the properties of certain semiconductor materials to effect the electron transfer processes in the cells like in the inner mitochondrial membrane.[29] The over production of the ROS beyond the tolerance capacity of the cell, results in impairment of normal physiological processes and modification of the structure of biomolecules.[30] ROS generation was studied by using cell permeable DCFH-DA (dichloro-dihydro-fluorescein diacetate) dye to measure the levels of oxidative stress within

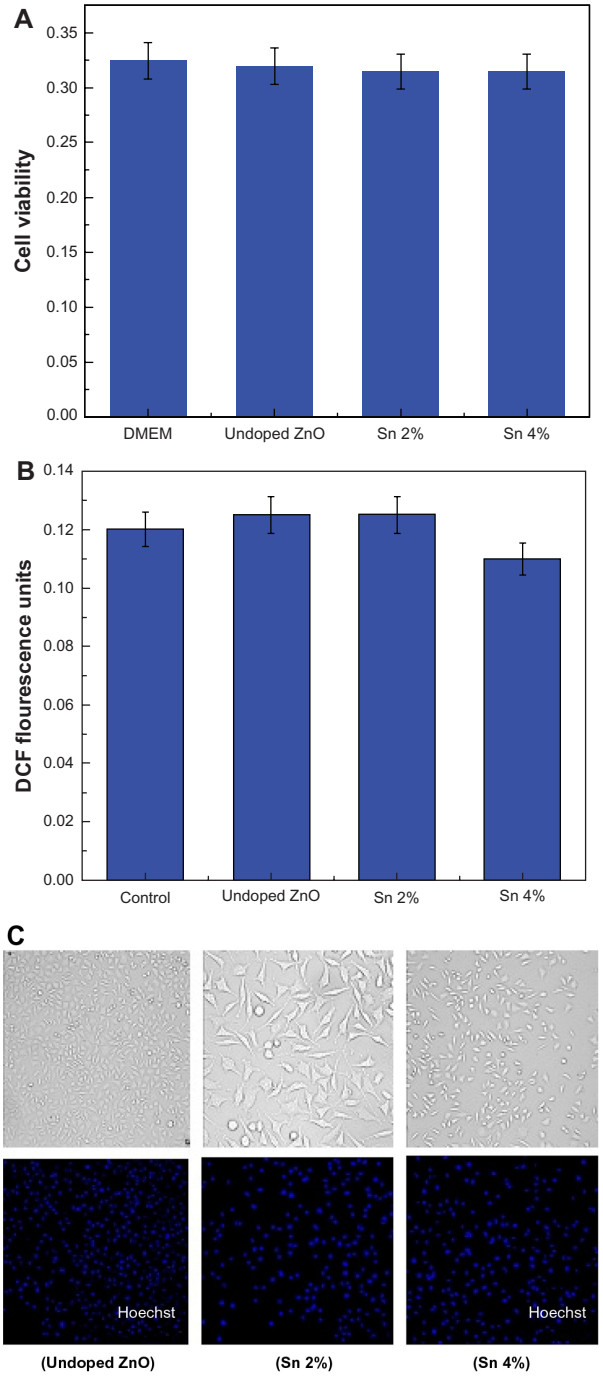

Figure 10 Effect of zinc oxide nanostructures on SH-SY5Y cells.
Notes: (**A**) Cell viability assay as a function of zinc oxide (ZnO) nanostructure doped with various concentration of tin (Sn). (**B**) Effect of Sn doped ZnO nanostructures on reactive oxygen species generation in SH-SY5Y cells. (**C**) Phase contrast microscopy of SH-SY5Y cells treated with undoped and Sn doped ZnO nanostructures.
Abbreviations: DMEM, Dulbecco's Modified Eagle's Medium; DCF, dihydrodichlorofluorescein; Sn, tin; ZnO, zinc oxide.

the cell. This dye can be diffused within the cell and can be oxidatively modified into a fluorescent derivative by different ROS, in particular superoxide anion and hydrogen peroxide in presence of certain cofactors. For the detection of levels of ROS production in SH-SY5Y cells and their morphology, flow cytometery was used. It has been shown in Figure 10B, that there is negligible amount of ROS production in SH-SY5Y cells which have been treated with undoped ZnO and Sn doped ZnO nanostructures.

It is also evident from Figure 10C, which was obtained by phase contrast microscopy, that cells are healthy and have normal morphology in the samples treated with undoped ZnO and Sn doped ZnO.

Conclusion

In this work, undoped ZnO and Sn doped ZnO have been successfully synthesized by a simple and cost effective coprecipitation technique. The detailed study reveals that all the synthesized samples are crystalline nanostructures with hexagonal wurtzite structure. The shift in the main diffraction peak (101), increase in the particle size, modification in morphology, and tailoring in the excitation absorption peak with increases in Sn concentration into ZnO clearly demonstrate the successful substitution of Sn dopant into the host matrix. The antibacterial assay and in vitro antibacterial activity of undoped and Sn doped ZnO nanostructures has been performed by optical density measurement and the disc method, respectively. It is observed from the in vitro test that Sn doping enhances the inhibitory activity of ZnO against *S. aureus* more efficiently than against the other two bacterial strains. It is concluded that Sn dopant content, particle size, and morphology play significant roles to influence the activity of ZnO nanostructures against all the bacterial strains tested. From the cytotoxicity and the ROS production study, it is concluded that Sn doping into ZnO does not alter the cytotoxicity and ROS production very much. The undoped and Sn doped ZnO nanostructures are biosafe and biocompatible materials toward SH-SY5Y cells.

Acknowledgment

The authors would like to acknowledge the financial support by Higher Education Commission (HEC), Pakistan through Indigenous 5000 Fellowships (T Jan), Interim Placement of Fresh PhDs Program (IPFP) Grant No: PM-IPFP/HRD/HEC/2011/3386 (J Iqbal), and National Research Program for Universities (NRPU) HEC project 20-2002 (R&D) at Quaid-i-Azam University (M Zakaullah).

Disclosure

The authors report no conflict of interest in this work.

References

1. Wu YL, Tok AIY, Boey FYC, Zeng XT, Zhang XH. Surface modification of ZnO nanocrystals. *Appl Surf Sci*. 2007;253:5473–5479.

2. Taccola L, Raffa V, Riggio C, et al. Zinc oxide nanoparticles as selective killers of proliferating cells. *Int J Nanomedicine*. 2011;6:1129–1140.
3. Yousefi R, Kamaluddin B. Effect of S- and Sn-doping to the optical properties of ZnO nanobelts. *Appl Surf Sci*. 2009;255:9376–9380.
4. Akhtar MS, Khan MA, Jeon MS, Yang OB. Controlled synthesis of various ZnO nanostructured materials by capping agents-assisted hydrothermal method for dye-sensitized solar cells. *Electrochim Acta*. 2008;53:7869–7874.
5. Morfa AJ, Kirkwood N, Karg M, Singh Th B, Mulvaney P. Effect of defects on the behavior of ZnO nanoparticle FETs. *J Phys Chem C*. 2011;115:8312–8315.
6. Akhtar MJ, Ahamed M, Kumar S, Khan MM, Ahmad J, Alrokayan SA. Zinc oxide nanoparticles selectively induce apoptosis in human cancer cells through reactive oxygen species. *Int J Nanomedicine*. 2012;7:845–857.
7. Jones N, Ray B, Ranjit KT, Manna AC. Antibacterial activity of ZnO nanoparticle suspensions on a broad spectrum of microorganisms. *FEMS Microbiol Lett*. 2008;279:71–76.
8. Salah N, Habib SS, Khan ZH, et al. High-energy ball milling technique for ZnO nanoparticles as antibacterial materials. *Int J Nanomedicine*. 2011;6:863–869.
9. Jung M, Kim S, Ju S. Enhancement of green emission from Sn-doped ZnO nanowires. *Opt Mater (Amst)*. 2011;33:280–283.
10. Ameen S, Akhtar MS, Seo HK, Kim YS, Shin HK. Influence of Sn doping on ZnO nanostructures from nanoparticles to spindle shape and their photoelectrochemical properties for dye sensitized solar cells. *Chem Eng J*. 2012;187:351–356.
11. Desselberger U. Emerging and re-emerging infectious diseases. *J Infect*. 2000;40:3–15.
12. Azam A, Ahmed AS, Oves M, Khan MS, Habib SS, Memic A. Antimicrobial activity of metal oxide nanoparticles against Gram-positive and Gram-negative bacteria: a comparative study. *Int J Nanomedicine*. 2012;7:6003–6009.
13. Vandenesch F, Naimi T, Enright MC, et al. Community-acquired methicillin-resistant Staphylococcus aureus carrying Panton-Valentine leukocidin genes: worldwide emergence. *Emerg Infect Dis*. 2003;9:978–984.
14. Hall-Stoodley L, Costerton JW, Stoodley P. Bacterial biofilms: from the natural environment to infectious diseases. *Nat Rev Microbiol*. 2004;2:95–108.
15. Ayeshamariam A, Tajun Meera Begam M, Jayachandran M, Praveen Kumar G, Bououdina M. Green synthesis of nanostructured materials for antibacterial and antifungal activities. *International Journal of Bioassays*. 2013;2:304–311.
16. Zhang LL, Jiang YH, Ding YL, Povey M, York D. Investigation into the antibacterial behavior of suspensions of ZnO nanoparticles (ZnO nanofluids). *J Nanoparticle Res*. 2007;93:479–489.
17. Sayilkana F, Asilturk M, Kiraz N, Burunkaya E, Arpac E, Sayilkan H. Photocatalytic antibacterial performance of Sn^{4+}-doped TiO_2 thin films on glass substrate. *J Hazard Mater*. 2009;162:1309–1316.
18. Jang YS, Lee EY, Park Y-H, et al. The potential for skin irritation, phototoxicity, and sensitization of ZnO nanoparticles. *Mol Cell Toxicol*. 2012;8:171–177.
19. Peng Z, Dai G, Zhou W, et al. Photoluminescence and Raman analysis of novel ZnO tetrapod and multipod nanostructures. *Appl Surf Sci*. 2010;256:6814–6818.
20. Kripal R, Gupta AK, Srivastavab RK, Mishra SK. Photoconductivity and photoluminescence of ZnO nanoparticles synthesized via co-precipitation method. *Spectrochim Acta A Mol Biomol Spectrosc*. 2011;79:1605–1612.
21. Luo L, Hafliger K, Xie D, Niederberger M. Transparent conducting Sn:ZnO films deposited from nanoparticles. *J Sol-Gel Sci Technol*. 2013;65:28–35.
22. Prasad V, D'Souza C, Yadav D, Shaikh AJ, Nadanathangam V. Spectroscopic characterization of zinc oxide nanorods synthesized by solid-state reaction. *Spectrochim Acta A Mol Biomol Spectrosc*. 2006;65:173–178.
23. Wu L, Wu Y, Pan X, Kong F. Synthesis of ZnO nanorod and the annealing effect on its photoluminescence property. *Opt Mater*. 2006;28:418–422.
24. Gunalan S, Sivaraj R, Rajendran V. Green synthesized ZnO nanoparticles against bacterial and fungal pathogens. *Progress in Natural Science: Materials International*. 2012;22:693–700.
25. Yamamoto O. Influence of particle size on the antibacterial activity of zinc oxide. *International Journal of Inorganic Materials*. 2001;3:643–646.
26. Tam KH, Djurisic AB, Chan CMN, et al. Antibacterial activity of ZnO nanorods prepared by a hydrothermal method. *Thin Solid Films*. 2008;516:6167–6174.
27. Schwartz VB, Thetiot F, Ritz S, et al. Antibacterial surface coatings from zinc oxide nanoparticles embedded in poly(*N*-isopropylacrylamide) hydrogel surface layers. *Adv Funct Mater*. 2012;22:2376–2386.
28. Lipsky BA, Tabak YP, Johannes RS, Vo L, Hyde L, Weigelt JA. Skin and soft tissue infections in hospitalised patients with diabetes: culture isolates and risk factors associated with mortality, length of stay and cost. *Diabetologia*. 2010;53:914–923.
29. Xia, T, Kovochich, M, Liong M, et al. Comparison of the mechanism of toxicity of zinc oxide and cerium oxide nanoparticles based on dissolution and oxidative stress properties. *ACS Nano*. 2008;10:2121–2134.
30. Hanley C, Thurber A, Hanna C, Punnoose A, Zhang J, Wingett DG. The influences of cell type and ZnO nanoparticle size on immune cell cytotoxicity and cytokine induction. *Nanoscale Res Lett*. 2009;4:1409–1420.